Discriminant Brain Connectivity Patterns of Performance Monitoring at Average and Single-Trial Levels

Huaijian Zhang, Ricardo Chavarriaga, José del R. Millán

PII: S1053-8119(15)00621-7
DOI: doi: 10.1016/j.neuroimage.2015.07.012
Reference: YNIMG 12401

To appear in: *NeuroImage*

Received date: 8 January 2015
Accepted date: 6 July 2015

Please cite this article as: Zhang, Huaijian, Chavarriaga, Ricardo, Millán, José del R., Discriminant Brain Connectivity Patterns of Performance Monitoring at Average and Single-Trial Levels, *NeuroImage* (2015), doi: 10.1016/j.neuroimage.2015.07.012

Title

Discriminant Brain Connectivity Patterns of Performance Monitoring at Average and Single-trial Levels

Author Names and Affiliation

Names: Huaijian Zhang, Ricardo Chavarriaga, and José del R. Millán

Affiliation:

Defitech Foundation Chair in Brain-Machine Interface,
Center for Neuroprosthetics,
École Polytechnique Fédérale de Lausanne (EPFL)

Corresponding Author

José del R. Millán
School of Engineering
EPFL STI-CNBI
ELB 138
Station 11
CH-1015 Lausanne

Email: jose.millan@epfl.ch
Phone: +41(0)21 693 5311

Acknowledgements

This study is supported by Nissan Motor Co. Ltd., and carried out under the “Research on Brain Machine Interface for Drivers” project. We thank Mohit Kumar Goel for his help on performing some of the experiments.

Electrophysiological and neuroimaging evidence suggest the existence of common mechanisms for monitoring erroneous events, independent of the source of errors. Previous works have described modulations of theta activity in the medial frontal cortex elicited by either self-generated errors or erroneous feedback. In turn, similar patterns have recently been reported to appear after the observation of external errors. We report cross-regional interactions after observation of errors at both average and single-trial levels. We recorded scalp electroencephalography (EEG) signals from 15 subjects while monitoring the movement of a cursor on a computer screen. Connectivity patterns, estimated using multivariate auto-regressive models, show increased error-related modulations of the information transfer in the theta and alpha bands between frontocentral and frontolateral areas. Conversely, a decrease of connectivity in the beta band is also observed. These network patterns are similar to those elicited by self-generated errors. However, since no motor response is required, they appear to be related to intrinsic mechanisms of error processing, instead of being linked to co-activation of motor areas. Noticeably, we demonstrate that cross-regional interaction patterns can be estimated on a trial-by-trial basis. These trial-specific patterns, consistent with the multi-trial analysis, convey discriminant information on whether a trial was elicited by observation of an erroneous action. Overall, our study supports the role of frequency-specific modulations in the medial frontal cortex in coordinating cross-regional activity during cognitive monitoring at a single-trial basis.

Keywords: Monitoring error; EEG; brain connectivity; anterior cingulate cortex; single-trial classification; multivariate auto-regressive model.

I. Introduction

The monitoring of erroneous events is an essential function of the human brain for behavior adjusting and learning (Holroyd and Coles, 2002; Taylor, Stern, and Gehring, 2007). Converging evidence from electroencephalography (EEG) and functional magnetic resonance imaging (fMRI) studies suggests that common neural mechanisms are involved in monitoring self-generated errors –when subjects make wrong decisions in response to cues– as well as when they observe erroneous external events or feedbacks (van Schie et al., 2004; Cavanagh, Zambrano-Vazquez, and Allen, 2012; Ullsperger et al., 2014). The medial frontal cortex (MFC), and more specifically the anterior cingulate cortex (ACC) has been suggested as the putative locus of these mechanisms (Milner et al., 2004; de Bruijn et al., 2009; Shane et al., 2008). Activity in this area has been reported to be sensitive to expectation mismatch, error of motor commission, and erroneous feedback, reflecting both endogenous and exogenous performance-relevant information (Cavanagh, Zambrano-Vazquez, and Allen, 2012). The present work focuses on the monitoring of external events and reports evidence of functional brain connectivity patterns both at average and single trial levels that support the similarity of neural process between monitoring external and self-generated events.

The electrophysiological signature of these monitoring processes appears as an event-related potential (ERP) over frontocentral areas elicited by both self-generated and external errors (Cavanagh, Zambrano-Vazquez, and Allen, 2012; Ullsperger et al., 2014). In the former case, the ERP shows an early negative deflection, termed as error-related negativity (ERN), appearing no later than 120 ms after the erroneous motor response (Gehring et al., 1993). The monitoring of external events elicits a similar modulation around 250 ms after stimuli (feedback-related negativity, FRN). Despite the timing difference, the negativities in both conditions precede a frontocentral positive deflection, followed by a sustained positivity over parietal areas (Ullsperger et al., 2014). Furthermore, source analysis of scalp ERP signals suggests that the brain systems associated with the monitoring of self-generated errors are also activated by the process of monitoring external errors (van Schie et al., 2004).

EEG activity after self-generated errors exhibits response-locked theta band modulations at the ACC (Luu, Flaisch, and Tucker, 2000; Trujillo and Allen, 2007; Cavanagh, Zambrano-Vazquez, and Allen, 2012). This region is believed to coordinate local and distant functional brain connectivity with other cortices for monitoring error events (Luu, Flaisch, and Tucker, 2000; Ullsperger and von Cramon, 2001; Brown and Braver, 2005). In particular, there exists strong evidence of causal influences from ACC to the lateral prefrontal cortex (LPFC) via increased theta activity (Luks et al., 2002; Brázdil et al., 2007; Cavanagh, Cohen, and Allen, 2009; Brázdil et al., 2009). Further studies in goal-directed behavior suggest that the ACC detects conflicting or unmatched information and notifies the LPFC and other related cortices as part of a monitoring system (Carter et al., 2000; Luks et al., 2002; Kerns et al., 2004). Moreover, both scalp EEG and magnetoncephalography (MEG) studies have shown increased amplitude of theta interactions (Cavanagh, Cohen, and Allen, 2009; Brázdil et al., 2009), as well as beta rhythm suppression after the monitoring of erroneous responses (Cohen et al., 2008; Koelewijn et al., 2008; Mazaheri et al., 2009). These studies provide a consistent depiction of the connectivity patterns related to the monitoring of self-generated errors.

Complementing these works, in this study we analyze the brain connectivity patterns generated by the process of monitoring external errors. Our results show frequency-specific modulations of connectivity patterns in frontocentral and frontolateral areas consistent with those observed after subject-generated errors, thus supporting the role of cross-regional activity modulations in the theta band during the observation of external conflicts. Moreover, we show that beta modulations also appear after the observed errors, and are not exclusive to motor-related tasks. Last but not least, we demonstrate that connectivity patterns can be estimated on a single-trial basis. The resulting patterns are consistent with the multi-trial analysis and, remarkably, carry discriminant information about whether or not a trial corresponds to an erroneous action. Furthermore, connectivity-based patterns are shown to convey complementary information to temporal features.

II. Materials and Methods

Participants and experiment procedure

Fifteen subjects (4 females, mean age 27.13 ± 2.59) participated in the experiments. All subjects had normal or corrected-to-normal vision, and did not report any known neurological or psychiatric disease. Subjects were asked to monitor whether a cursor on a computer screen moved towards a given target. This protocol has been previously shown to elicit error-related potentials in the frame of brain-machine interfacing (Chavarriaga and Millán, 2010; Iturrate et al., 2014). Subjects seated in front of a computer screen located at 50 cm from their eyes. During the experiment 20 light red squares were shown along a horizontal line in the center of the screen. At the beginning, one of the squares either at the left- or the right-most position turns red to indicate the target position (preferred direction), and one of the other squares turns green and becomes the moving cursor. The initial cursor position was chosen randomly, but at least two steps away from the target. At each trial, the cursor square moved one position either left or right, with 80% probability of approaching the target, and remained at its new position for 2000 ms before moving again. A correct trial is defined when the cursor moves towards the target, whereas trials where it moved in the opposite direction are labeled as error trials. The cursor and the target were relocated at random positions when the cursor reached the target or if 10 steps were performed without reaching it. During the experiments, subjects were requested to minimize eye blinking and movements. Each trial corresponds to a single cursor movement, and recordings yielded about 400 correct and 100 error trials for each subject. For all the subjects, the target was reached 94.27 $\pm$ 33.24 (mean $\pm$ standard deviation) times on average, whereas it was not reached in 6.60 $\pm$ 4.95 occasions. Since the location of the target was randomized, the moving directions of cursor (left or right) for both conditions were balanced and uncorrelated to the trial type (i.e., correct or error). Moreover, previous studies using this protocol have shown that ERPs are not correlated to the target position or to eye movements (Ferrez and Millán, 2008; Chavarriaga and Millán, 2010).

EEG recording and pre-processing

Scalp EEG was recorded using 64 electrodes (Biosemi Active Two, The Netherlands) with an extended 10-20 system montage at a sampling rate of 2048 Hz. The EEG signals were downsampled to 512 Hz. We filtered the EEG data in the frequency band [1, 50] Hz with a 4^{th} order non-causal Butterworth filter. Afterwards, EEG data were epoched into trials, corresponding to cursor movements either correct or erroneous. Each trial lasted 2 s, from 1 s before the onset of the action to 1 s after.

Before estimating the connectivity patterns, we computed current source density (CSD) from the EEG signal to reduce the effect of volume conduction (Kayser and Tenke, 2006). This avoids spurious bi-directional brain connectivity patterns (Kayser and Tenke, 2006). CSDs are estimated by the second spatial derivative of the potential between electrodes, thus giving prominence to local activity and attenuating common distal activity which is usually considered as volume conduction (Kayser and Tenke, 2006).

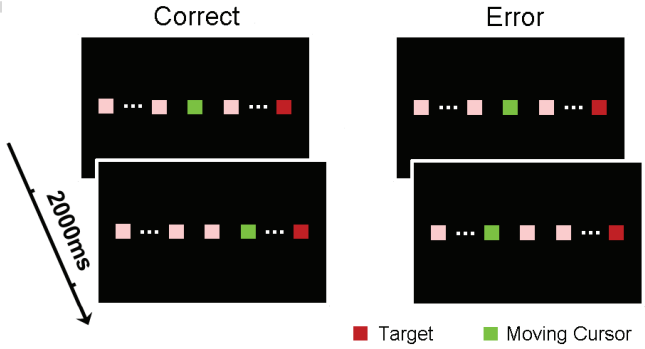

Fig. 1. Experimental protocol. 20 squares in light red are presented in a computer screen in front of the subject. The green square indicates the moving cursor and the red square represents the target. The green cursor moves to the target with 80% probability, i.e., correct trials (in the left column). The position of the moving cursor is randomly initialized after reaching the target (the target turned to light green) or continuing moving for more than 10 steps. The moving cursor stops on each position for 2000 ms.

Multi-trial brain connectivity

The brain connectivity patterns were computed both at the subject level and single-trial level. At the subject level, we explored the dynamics of the modulation with high temporal resolution between broad brain regions using multiple trials to increase the reliability of the estimated patterns. When analyzing the single-trial connectivity, we also assessed the feasibility of estimating discriminant connectivity patterns between a subset of channels selected from the results at the subject level.

The multi-trial connectivity between CSDs was computed using the short time direct directed transfer function (SdDTF) (Korzeniewska et al., 2008). This method is a modification of the directed transfer function (DTF), based on the estimation of a multivariate autoregressive model (MVAR). Defining $X_t = [x_{1,t}, x_{2,t}, \cdots, x_{k,t}]^T$ to be a vector of EEG samples of k channels at time point t (superscript T denotes matrix transposition), the MVAR model can be represented as

$$\sum_{j=0}^{p} A_j X_{t-j} = E_t \tag{1}$$

where E_t is a vector of zero-mean white noise with size $1 \times k$, and A_j is the $k \times k$ coefficient matrix with $A_0 = -I$ (I is the identity matrix). Here, p is the model order, indicating how many previous points are used to estimate the current sample. We used the Matlab package arfit (Schneider and Neumaier, 2001) to compute the coefficient matrices. Using Fourier transform, we investigate the relations in the frequency domain $X^F = H^F E^F$, where $H^F = (A^F)^{-1}$ and A^F is the Fourier transform of the coefficient matrix. The non-normalized DTF is defined by the system transfer matrix H^F, where $\theta_{ij}^2(f) = |H_{ij}^F(f)|^2$ represents the information transfer from channel j to i at f Hz (Kamiński and Blinowska, 1991).

We focused on estimating the connectivity patterns in short time windows around and after the cursor movement to identify brain modulation patterns during error processing. To this purpose we applied the multi-trial analysis assuming that the EEG signal is quasi-stationary over the window of interest, and estimated the coefficient matrix by averaging the covariance matrix across trials in each condition (Kamiński et al., 2001). This contributes to preserve the reliability of the parameter estimation even when short windows are selected (i.e., having a small number of data samples) or a large number of channels are taken in consideration (i.e., increasing number of parameters).

Additionally, partial coherence was used to avoid indirect cascade influences in the network, i.e., influences between two channels mediated by a third channel. The short time direct DTF (SdDTF) (Korzeniewska et al., 2008) is thus defined as:

$$\zeta_{ij}^{F}(f) = \frac{|H_{ij}^{F}(f)||\chi_{ij}^{F}(f)|}{\sum_f \sum_{ij} |H_{ij}^{F}(f)|^2 |\chi_{ij}^{F}(f)|^2}, \qquad (3)$$

where $\chi_{ij}^{F}(f)$ indicates the partial coherence (elements of the inverse of spectral matrix, $H^F V H^{F*}$, where V is the covariance of the noise term E^F) and the denominator is a normalization term across channels and frequencies. SdDTF values range from 0 to 1. The asymmetry of the matrix reflects the directionality of the cross-channel influences. One should also notice that the SdDTF reflects the phase difference between channels, thus the elements of the matrix are non-zero only when there exists a phase difference between them. In consequence, this measurement is insensitive to volume conduction (Blinowska, 2011).

In the multi-trial analysis, we estimate connectivity patterns within sliding windows of 250 ms with 90% overlapping. 41 CSDs were considered for the analysis, excluding the most peripheral electrodes, i.e., AF3, F1, F3, F5, FC5, FC3, FC1, C1, C3, C5, CP5, CP3, CP1, P1, P3, P5, PO3, POz, Pz, CPz, AF4, AFz, Fz, F2, F4, F6, FC6, FC4, FC2, FCz, Cz, C2, C4, C6, CP6, CP4, CP2, P2, P4, P6 and PO4. We used the same number of trials (100) for both correct and error conditions, as otherwise the order of the autoregressive model of the two conditions may be different. The 100 error/correct trials used in the analysis are uniformly distributed across the duration of the experiments. Before computing the MVAR model, we normalized the data within each sliding window (subtracting the mean and dividing the standard deviation within the window) for each CSD before computing the SdDTF to meet the zero mean requirement of the MVAR model (Kamiński and Blinowska, 1991). After that, data in each sliding window was also normalized across trials for each time sample to avoid spurious connectivity (Korzeniewska et al., 2008; Oya et al., 2007). The order of the model was determined by Schwarz's Bayesian Information Criterion (BIC) and the logarithm of Akaike's final prediction error using arfit (Schneider and Neumaier, 2001). Despite small variations, this resulted in a minimal order of about 10 for most sliding windows. We therefore fixed the model order to this value for both error and correct conditions on all subjects, so as to keep the same size of the coefficient matrices.

We identify brain regions that exhibit high levels of interaction by estimating the total information inflow and outflow at each location. The information inflow (outflow) at one point was defined as the sum of resulted SdDTF values from (to) all the other channels, or the total received (sent) information amount. For a given channel i and frequency f, we compute these values as $inflow = \sum_j \zeta_{ij}^{F}(f)$ ($outflow = \sum_j \zeta_{ji}^{F}(f)$). Given the prominent role of the theta oscillations in monitoring processes (Cavanagh, Zambrano-Vazquez, and Allen, 2012), we estimated the inflow and outflow of theta band in the error condition to determine the most active brain regions for the statistical analysis. Furthermore, this information was also used to select the subset of channels on which the single-trial analysis is performed (see below).

Statistical analysis

In the multi-trial level, we analyzed the statistical significance among the regions of interest, i.e., the subsets of electrodes selected according to the results of the inflow/outflow analysis. We computed the SdDTF between -875 ms and 875 ms (window size of 250 ms) from 1 Hz to 50 Hz. When reporting our results sliding windows are referred to by the time of its center point. The SdDTF values were divided by the average of the pre-stimulus activity (-875 ms to -125 ms) with the purpose of canceling out the variations across subjects. To assess the role of different frequency ranges, we analyzed the statistical significance in four bands following their common definitions, i.e., theta (4-8 Hz), alpha (8-13 Hz), beta (13-30 Hz) and gamma (30-50 Hz). Seven time windows were specified, including the baseline activity (-875 ms to -125 ms, whose value is 1 after normalization) and six windows at the moment of and after stimulus presentation (i.e., -100 to 100 ms, 0 to 200 ms, 100 to 300 ms, 200 to 400 ms, 300 to 500 ms and 400 to 600 ms), in order to verify the temporal evolution of significant brain connectivity modulations caused by the monitoring processes. After obtaining the average value of SdDTF in these time-frequency blocks (baseline/monitoring phases and four frequency ranges), we used Wilcoxon signed rank test to assess the significance of the null hypothesis that there was no difference in connectivity patterns between baseline and each monitoring time window. The type I error of these multiple tests was corrected by permutation tests, in which we randomly shuffled the baseline window (-875 ms to -125 ms) and the other 6 time windows for 1000 times, and obtained the corrected p value as the percentage of those permutations having lower p value than the original test.

Single trial connectivity and classification

We further assessed the information conveyed by the connectivity patterns by evaluating whether such information can be used to discriminate between error and correct conditions in single trials. In this analysis, we preprocessed the data with a 4^{th} order causal Butterworth filter after downsampling to 512 Hz, as the single trial analysis will be further implemented in a real-time framework. To estimate connectivity on a single trial basis, we restricted the analysis to a smaller number of channels and a longer time window

since fewer data samples were available. In this case, the size of the time window used was 400 ms with an overlap of 360 ms. Four EEG electrodes located at the center of frontolateral, frontocentral and centroparietal regions, i.e., F3, F4, FCz and CPz, were included in the MVAR computation. These regions showed high levels of information inflow/outflow as reported in the results section. The order of the MVAR model was set to 5 for all subjects, satisfying the same criteria used for the multi-trial case. We used the non-normalized DTF (i.e., θ_{ij}^2) as features for classification without considering the indirect effects due to the fact that less electrodes were included which are less likely to produce critical cascading indirect effects. Moreover, the computational cost is highly reduced as it is not necessary to compute the inverse of the spectral matrix. As in the multi-trial analysis, brain connectivity values were divided by the pre-stimulus level (-800 ms to -200 ms). Then, statistically significant differences between baseline (-800 ms to -200 ms) and post-stimulus connectivity (200 ms to 400 ms) were assessed using the Wilcoxon signed rank test. Notice that, compared to the multi-trial analysis, different time periods had to be defined for the analysis since longer time windows were used for computing the DTF values.

Moreover, we compared the classification accuracy (error vs. correct) based on the connectivity patterns to the use of standard temporal features. To verify whether connectivity features provide extra information with respect to the temporal features we also assessed classification accuracy using both types of features combined. Linear discriminant analysis (LDA) was used to classify correct and error trials. Three sets of features were compared: (1) Temporal features, corresponding to the most common approach used for classification of these type of signals for brain-computer interfacing (Chavarriaga, Sobolewski, and Millán, 2014); (2) Brain connectivity features (θ_{ij}^2); (3) Combination of temporal and connectivity features. Temporal features were extracted from the same 4 electrodes utilized in the single trial connectivity analysis, between 200 ms and 700 ms after the stimulus onset. This yielded a total number of 52 (13 time samples$\times$4 channels) features. In the second case, for each trial we extracted features between [1-30] Hz in the same time range as above. Since this results in more than 10^4 features, we selected for classification the 50 highest ranked features according to their Fisher score. This score indicates the discrimination capability of each feature and is defined as $fs = |m_1 - m_2|/(s_1^2 + s_2^2)$, where m_k and s_k^2 are the mean value and the variance of class k, respectively. In the third case, both temporal and connectivity features were used (selected separately) and then fed into the classifier. We report the classification performance as the area under the specificity-sensitivity curve (AUC) computed using 10-fold cross-validation. To verify whether the classification performance was significantly better than chance level, we used a permutation test, through training classifiers using randomly shuffled labels. The procedure of generating random classifier was repeated for 1000 times, and for each of them we obtained its testing performance. The upper 95% percentile of the testing performance distribution was obtained and compared to the results of the original classifier. This assesses how likely it is to obtain the classification performance by chance alone.

III. Results

Event related potentials (ERP) and spectrogram

On average, we obtained 121.33 $\pm$ 15.43 (mean $\pm$ standard deviation) error trials and 441.33 $\pm$ 12.71 correct trials per subject. Figure 2.A shows the grand average ERP of correct and error trials of four electrodes (F3, F4, FCz and CPz). For visualization, we filtered the raw EEG data between [1-10] Hz after using common average reference across all 64 channels. Significant differences between two conditions are shown as green areas in the figure (t-test, Bonferroni correction).

ERPs in FCz and CPz (midline areas) show higher modulations than the other selected electrodes. A negative peak appears at about 240 ms in the error condition (Figure 2.A, black lines) in both FCz and CPz. After that, a positive peak is observed at about 330 ms with a following negative peak at about 420 ms in FCz and around 500 ms in CPz. In the correct condition (Figure 2.A, gray lines), both FCz and CPz include a positive peak at around 260 ms and a negative peak around 400 ms. Significant differences can be observed from 200 ms until 650 ms after the stimuli onset in both FCz and CPz. In the electrodes F3 and F4 (frontolateral sites), the most evident differences between correct and error are found at about 420 ms. At this time a negative deflection, lasting until about 500 ms, can be observed in the error condition (black line) but not in the correct condition (gray line). Significant differences could be found around 420 ms in both F3 and F4. These differences are larger at the left frontal areas (F3).

These results are consistent with previous studies of error monitoring with a similar protocol (Chavarriaga and Millán, 2010; Iturrate et al., 2014), and the negative peak in midline regions, particularly FCz, replicates negative ERP deflections reported by other error monitoring experiments (van Schie et al., 2004; Milner et al., 2004; Ullsperger et al., 2014).

Figure 2.B illustrates the ERP (error - correct) of EEG topographies during (0 ms) and after the stimuli (ERP peaks: 240 ms, 330 ms and 490 ms). No evident difference could be found at 0 ms. In contrast, we found a larger negativity for the error condition in medial central regions at 240 ms, followed by higher activity at 330 ms. Finally a larger negativity is also observed for the error condition in medial frontal regions at 480 ms. The spectrogram of channels F3, F4, FCz and CPz, computed using the short-time Fourier transform with window size 250 ms and overlapping 98%, is shown in Figure 2.C, error - correct. Frontal central (FCz) theta occurring around 250 ms seems to be the most prominent pattern. It appears in other channels (CPz, F4 and F3) as well but exhibiting a smaller amplitude than in FCz. The theta modulations finish before 500 ms. A second modulation, although not as strong as in the theta band, manifests in the lower beta band in FCz and CPz at around 400 ms. Statistically significant differences (Wilcoxon ranksum test, corrected by a 1000 random permutation test) were found in FCz, CPz and F3, between 200 and 500 ms in the [4-10] Hz frequency range.

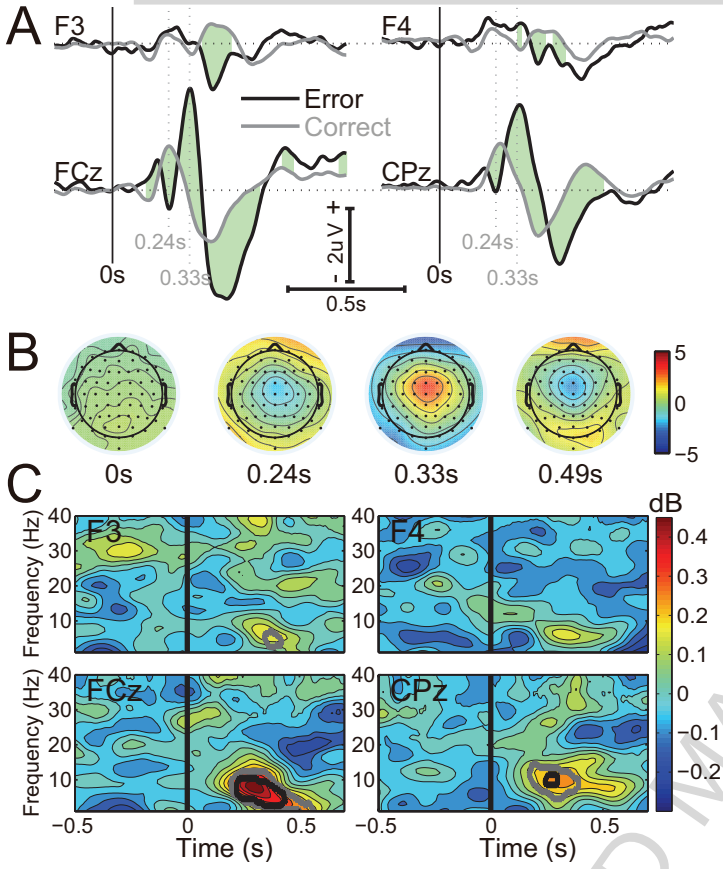

Fig. 2. A. Grand average of the event-related potential (ERP). The black lines indicate the error condition, the gray lines show the correct condition, and green areas show the periods with significant differences between error and correct. Origin of the time axis, 0 s, represents the onset of the visual stimuli (i.e. cursor movement). Four EEG channels in frontolateral (F3 and F4) and midline central (FCz and CPz) areas are illustrated. B. Topographies of the ERP difference (error - correct) at selected time points, -0.2 s, 0s, 0.24 s and 0.33 s. C. Differences of event related spectral perturbation of selected channels. The gray ($p < 0.05$) and black ($p < 0.01$) contours indicate the areas where significant differences between correct and error conditions were found.

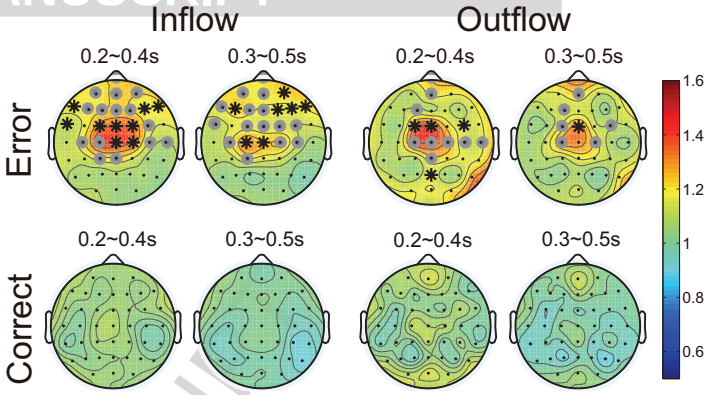

Fig. 3. Grand average of information inflow and outflow for all electrodes. Results were referenced by dividing the mean value of the pre-stimulus time window (-875 ms to -125 ms) and averaged for all subjects. Values equal to 1 denote no change from pre-stimulus levels. Greater values indicate an increase in inflow/outflow, while smaller values represents a decrease. Gray circles indicate $p < 0.002$, and the black markers denote statistical significance using Bonferroni correction.

Information inflow and outflow

Estimation of the information inflow and outflow shows that the error condition have stronger connectivity modulations than the correct condition (Figure 3). In the error condition, the frontal and frontocentral areas have the highest increased inflow. Most electrodes (gray circles, $p < 0.002$) in these regions show significant differences compared to the pre-stimulus activity, particularly in frontocentral and frontolateral channels, as shown by the black markers (Bonferroni correction). For the outflow patterns, the essential brain regions are frontocentral and centroparietal. In addition, given previous evidences that MFC is the generator of the error-related ERP (Holroyd and Coles, 2002; Taylor, Stern, and Gehring, 2007; Milner et al., 2004) and the contribution of frontoparietal interaction in the attention network (Ptak, 2012), we therefore choose frontocentral (defined as the combination of FC1, FCz and FC2 electrodes), frontolateral (F5, F3 and F1; and F6, F4 and F2 for left and right ones respectively) and centroparietal (CP1, CPz and CP2) regions for further analyses. We averaged the brain connectivity of electrode pairs between these regions after the computation of the SdDTF, e.g. the connectivity from frontocentral to left frontolateral is the mean value among all pairs from electrodes FC1, FCz and FC2 to electrodes F1, F3 and F5.

Multi-trial brain connectivity patterns

Figures 4.A, C and E illustrate the dynamics of directional brain connectivity patterns in the time-frequency domains. The statistical tests (Wilcoxon signed rank test) between baseline (-875 ms to -125 ms) and monitoring periods at a subject level are shown in Figure 4.B, D and F. As can be observed, significant differences only appeared in the error condition, specifically in the theta band.

In lower frequencies, i.e. theta and alpha, brain connectivity increases. In error trials, significant increases ($p < 0.05$) appear in the information flow from frontocentral to both left and right frontolateral areas in the theta band, starting at about 200 ms and ending at about 400 ms. Significant connectivity pattern between frontocentral and left frontolateral areas (Figure 4.A, 4.B, 4.C and 4.D) could also be observed. In contrast, no significant modulation appears after correct trials. The pattern of information flow in the opposite direction (i.e. from frontolateral to frontocentral sites) exhibits an increase in the theta and alpha band, and is significant from the right hemisphere ($p < 0.05$). In the correct condition, the brain connectivity in both directions does not change significantly neither in the theta nor alpha band ($p > 0.05$) with respect to the baseline period. The information flow from centroparietal to frontocentral areas shows an early increase (starting at about 100 ms) in connectivity in the theta band for the error condition, as displayed in Figures 4.E and F. This modulation precedes those observed between frontocentral and frontolateral regions, and may be related to perceptual processes. An increase in connectivity from frontocentral to centroparietal areas appears in the alpha and theta bands as well.

In higher frequency bands, i.e. beta and gamma, we observe a significant decrease in the information flow from frontolateral to frontocentral areas in the error condition. This pattern slightly precedes the increase observed in lower frequencies. This pattern is significant in the error con-

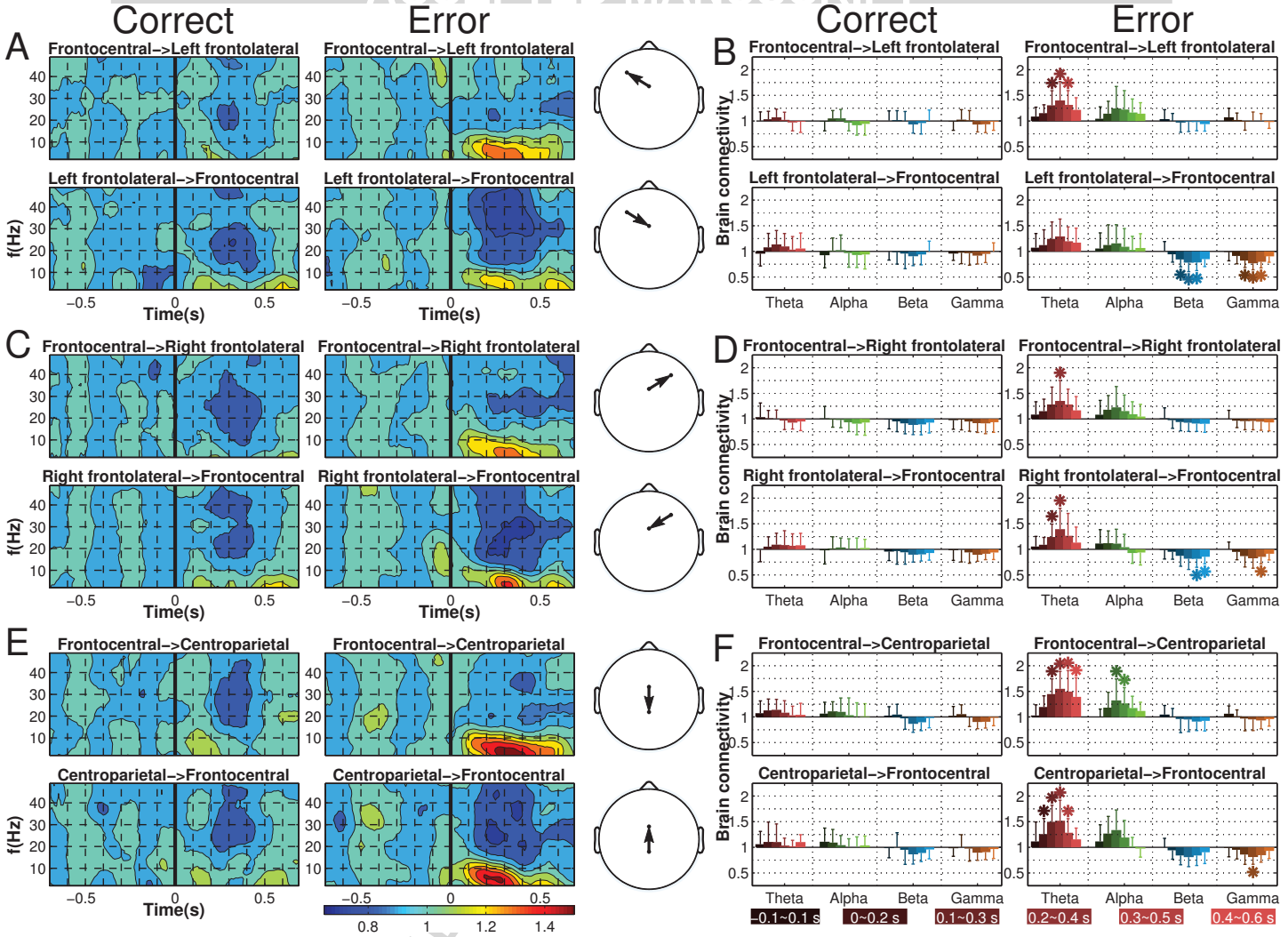

Fig. 4. Brain connectivity between frontocentral, frontolateral and centroparietal areas. A, C and E represent SdDTF in the time-frequency domain. Colors in the figure represent the ratio with respect to pre-stimulus level (average between -875 s and -125 ms). Values equal to 1 represents no difference (equivalent as pre-stimulus level) in brain connectivity. Smaller values indicate depressed brain connectivity, and, conversely, values greater than 1 denotes enhanced cross-regional interactions. The two columns on the right side (B, D and F) show the mean values and standard deviations of the SdDTF for each window and frequency band across subjects. The duration of the six windows are indicated at the bottom of the two right-side columns ([-0.1, 0.1], [0.0, 0.2], [0.1, 0.3], [0.2, 0.4], [0.3, 0.5] and [0.4, 0.6]). They also indicate significant differences (Wilcoxon signed rank test, $p < 0.05$). The head maps in the center line indicate the brain regions that are analyzed: frontocentral and left frontolateral in A and B; frontocentral and right frontolateral in C and D; frontocentral and centroparietal in E and F.

dition ($p < 0.05$) between baseline and after onset: starting at 100 ms to 300 ms from left side in beta and gamma and later from the right hemisphere. As before, no significant modulations appear in the correct condition.

Information flow in the opposite direction, from frontocentral to frontolateral areas, decreases as compared to the baseline level for both conditions, but no significant change could be found. The connectivity patterns between frontocentral and centroparietal regions also decrease in the error condition, with a significant reduction from centroparietal to frontocentral in the gamma band ($p < 0.05$). As before, the modulations in the correct condition are much lower and show no significant difference with respect to baseline levels.

Single trial connectivity and classification

Figure 5.A shows the estimation of the single trial modulation of brain connectivity patterns between F3, F4, FCz and CPz. The figure illustrates the grand average of all trials of the 15 subjects in the time window 200 ms to 400 ms as well as statistically significant values with respect to the baseline period (-800 to -200 ms).

The connectivity values of the correct condition (gray bars) show no significant modulation, in comparison to the baseline period. In the error condition, the results are consistent with the multi-trial analysis, i.e. information flows from frontocentral to frontolateral and centroparietal sites are enhanced in the theta band. A decrease in beta connectivity in the opposite direction is also observed, which is significant from frontolateral to frontocentral sites.

We computed the Fisher score for each connectivity feature, which measures how well that feature separates correct and error trials. Figure 5.B reports the averaged Fisher score of all pairs throughout the frequency domain for each time point. The Fisher score revealed that most of the discriminability between error and correct trials came from the time interval between 200 ms to 400 ms. Figure 5.C shows an equivalent analysis in the frequency domain.

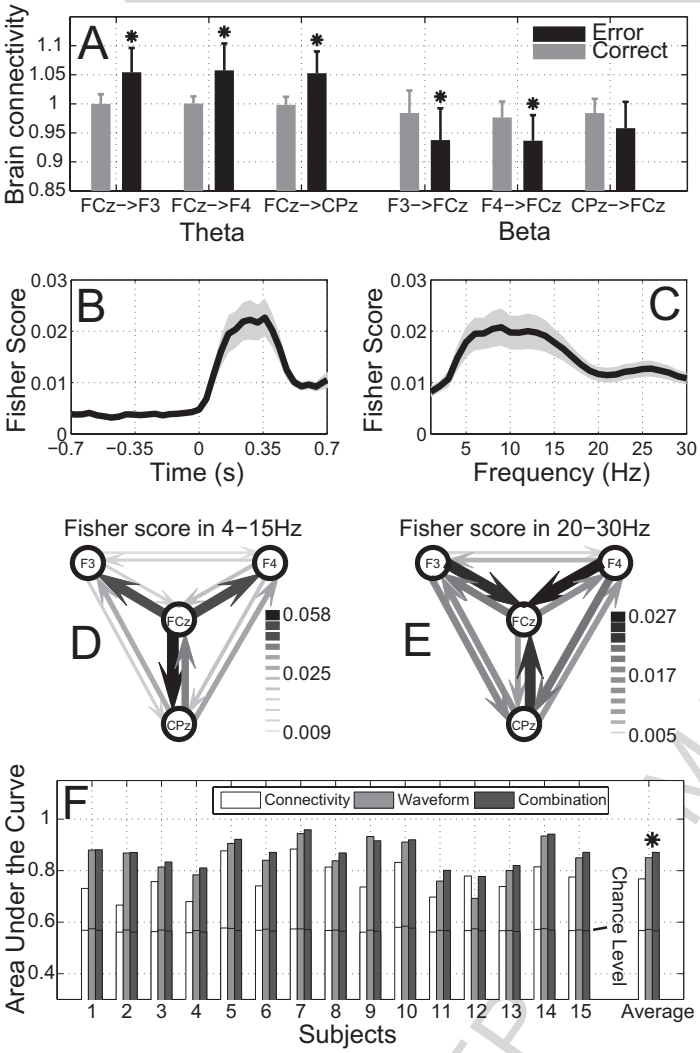

Fig. 5. Single trial analysis of brain connectivity between F3, F4, FCz and CPz. A. The columns represent the mean value between 200 ms and 400 ms for theta and beta bands. Asterisks indicate statistical significance ($p < 0.05$) between baseline (-800 ms to -200 ms) and after onset (200 ms to 400 ms). B. Discrimination power (Averaged Fisher score $\pm$ standard error) of brain connectivity features in temporal domain. C. Discrimination power of brain connectivity features (Averaged Fisher score $\pm$ standard error) in frequency domain. D and E: Spatial directionality of discrimination power in low (4-15 Hz) and high (25-30 Hz) frequency bands. The width of the arrows represents the normalized Fisher score. F. Classification performances of three feature sets: connectivity, temporal and the combination of them. The bars represent AUC for each subject, and the black lines indicate the 95% confidence chance of output from random classifiers. Asterisk indicates that, across all subjects, the combination of features yields a significant improvement ($p < 0.05$, see text for details).

Low frequency bands (4-15 Hz, mainly theta and alpha) are the most dominant rhythms, with a smaller peak in beta (around 25 Hz). Discrimination power associated to spatial directionality (averaged in time window 0 s-0.7 s) are illustrated in Figures 5.D and 5.E for 4-15 Hz and 25-30 Hz, corresponding to the two peaks in Figure 5.C. The width of the arrows represents the normalized Fisher score. The information flows in the theta band from FCz to F3, F4 and CPz are much stronger than others, while a larger decrease is seen in the beta flows from F3, F4 and CPz to FCz. These results are consistent with the patterns obtained in the multi-trial analysis.

Figure 5.F shows the classification performance (AUC) for the three types of features used: connectivity, temporal and combined features. Besides the AUC for each subject it also shows the mean AUC across all subjects. Chance level estimated using a permutation test (95% confidence interval) is indicated by the black line in the bar. In all subjects the three types of features yielded classification performance significantly higher than chance level (paired Wilcoxon signed rank test $p<0.05$). The performance using connectivity-based features (AUC = 0.7682) was lower than for temporal features (AUC = 0.8502). However, the combination of the two features resulted in significantly higher performance (AUC = 0.8709) than using temporal features alone (paired Wilcoxon signed rank test, $p<0.05$). Overall, 14 out of 15 subjects had higher AUC with combined features. These results suggest that not only it is feasible to extract discriminant information from the connectivity patterns in single trials, but also that this information is complementary to the customary temporal features.

Methodological Considerations

The brain activity at source level is particularly interesting. For this, inverse solution methods are usually used to estimate the source activity prior to the connectivity analysis (Schoffelen and Gross, 2009; Hipp, Engel, and Siegel, 2011). As a methodological check, we include it in this study. Among the existent inverse solution methods, beamforming is one of the most frequently used methods. This method maps the EEG signals into electric activities within specific regions of interest (ROI) by maximizing the variance ratio inside and outside the ROI (Grosse-Wentrup et al., 2009). We replicated the previous analysis using this technique. The processing followed the computational steps in (Grosse-Wentrup et al., 2009), and we used the generic MNI-based leadfield matrix for all subjects. ROIs were selected as the 10 closest voxels (within 1.5 cm radius sphere from the closet point in the cortex under the surface electrode) to each of the 41 EEG electrodes. Particularly, the beamformer was derived for each subject using 100 trials (-1 s to 1 s) in both conditions together. Figure 6.A shows the averaged source topographies (error - correct) at the ERP peaks, 240 ms and 330 ms. Consistent patterns with the EEG topographies were found (Figure 2.B), i.e. negativity at 240 ms and positivity at 330 ms in medial central areas. The spectrogram (error - correct) of the four selected ROIs, under F3, F4, FCz and CPz, are illustrated in Figure 6.B, showing higher theta modulation in the error condition from about 200 ms after stimulus onset. We also estimated single-trial connectivity patterns between the four selected ROIs, i.e. left and right frontolateral, medial frontal and centroparietal regions, using DTF. This yielded similar brain connectivity patterns (measured by the Fisher scores, Figure 6.C), particularly in the theta band. The colors of the head model indicate the differences (error - correct) of the band power, theta (left) and beta (right) in all 41 ROIs, showing higher theta and lower beta power in the error condition.

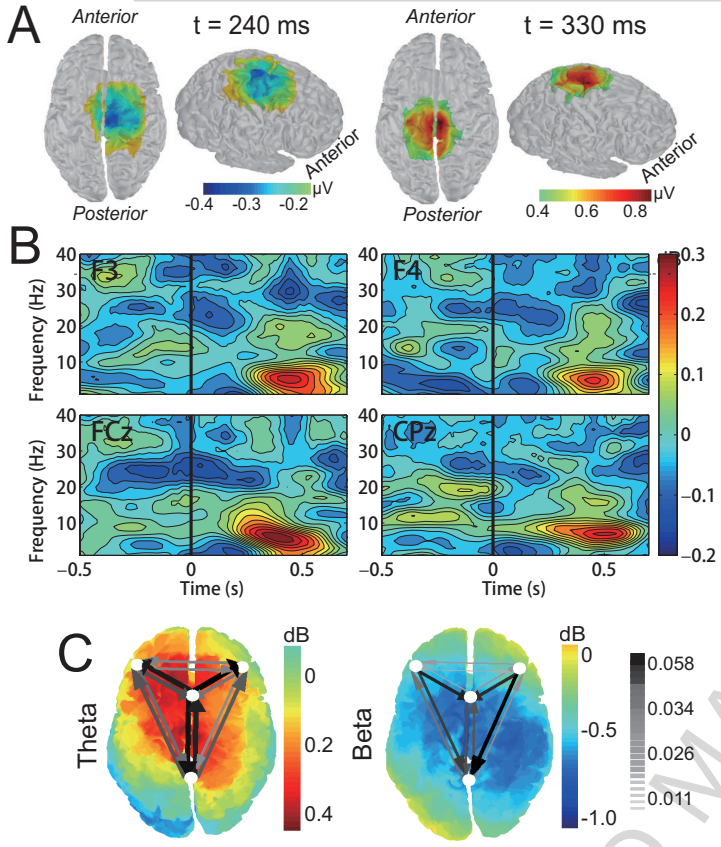

Fig. 6. A. The difference (error - correct) of topographies in source level at 240 ms and 330 ms after visual stimuli, using beamforming of 41 ROIs under 41 central EEG electrodes. The values are thresholded at -0.2 μV for the negative peak and 0.4 μV for the positive peak. B. Time-frequency spectrogram (error - correct) of four brain sources under electrodes F3, F4, FCz and CPz. C. Fisher score of brain connectivity patterns between four selected brain sources, in two frequency bands, 4-15 Hz and 20-30 Hz. The values of the Fisher score are represented by the color and the thickness of the arrows. Power spectrum density (error - correct) of the brain sources at 240 ms is indicated by the color.

IV. Discussion

The results of the current work show that specific modulations of directional brain connectivity patterns are elicited when subjects are monitoring external erroneous events. In particular, there is an increase of information transfer at the theta band between frontal and parietal regions and from frontocentral to frontolateral areas; as well as a suppression of brain interactions from frontolateral and centroparietal to frontocentral areas at the beta band. Previous studies using intracranial and surface EEG, as well as hemodynamics neuroimaging techniques have pointed out that the information transfer patterns between the frontolateral and frontocentral regions are associated with the monitoring of self-generated errors (Cavanagh, Cohen, and Allen, 2009; Brázdil et al., 2009; Debener et al., 2005). In addition, there are consistent reports of MFC activation due to erroneous information both from internal and external sources (Holroyd et al., 2004; Cavanagh, Zambrano-Vazquez, and Allen, 2012). We report patterns similar to those obtained for monitoring self-generated errors, further supporting the existence of a common mechanism of monitoring processes in the brain, irrespective of the modality of the error.

Theta dynamics in the MFC relates to focused attention, working memory and action control (Klimesch, 1999; Klimesch et al., 2001; Sauseng et al., 2004; Gevins and Smith, 2000; Buzsáki and Draguhn, 2004), particularly error monitoring and feedback processing in both human (Trujillo and Allen, 2007; Cavanagh, Cohen, and Allen, 2009; Cohen et al., 2008; Wang et al., 2005) and primates (Tsujimoto et al., 2010; Womelsdorf et al., 2010; Kuwabara et al., 2014), and organize cross-regional brain interactions for cognitive control processes (Cohen and Cavanagh, 2011; Cohen et al., 2009). Further studies report the MFC theta as a common temporal neural pattern during endogenous and exogenous monitoring processes (Cavanagh, Zambrano-Vazquez, and Allen, 2012; Ullsperger et al., 2014). We report increased theta connectivity patterns during error monitoring. In particular, the directional information transfers from frontocentral to frontolateral regions possibly reflect the communication from MFC to lateral regions as further cognitive reaction after the error detection in MFC, consistent with the patterns elicited by self-generated errors as measured by electrophysiological (Luks et al., 2002; Brázdil et al., 2007; Cavanagh, Cohen, and Allen, 2009; Brázdil et al., 2009), and fMRI (Debener et al., 2005; Agam et al., 2011) techniques. This highlights the role of theta dynamics in frontal areas as a common cognitive mechanism between different performance monitoring processes, i.e., external erroneous events and self-generated errors (Cavanagh, Zambrano-Vazquez, and Allen, 2012).

Interestingly, we found stronger information flow from frontocentral to left frontolateral than from frontocentral to right regions, illustrated in Figure 4. The lateralization phenomenon is also observable in ERP amplitudes, where the F3 has lower negative peak than F4, as shown in Figure 2. A. Larger inter-channel theta synchrony between left frontal hemisphere and frontocentral sites – with respect to right frontolateral sites – have been previously reported in action monitoring tasks, c.f., Figure 3 in (Cavanagh, Cohen, and Allen, 2009). It has been suggested that the left dorsal prefrontal cortex is more related to participant's expectation regarding the nature of the upcoming trial, whereas the right dorsal prefrontal cortex is associated with the online macro-adjustments in a conflict-driven context (Vanderhasselt, Raedt, and Baeken, 2009). It might be possible that the pattern of lower interactions with right frontocentral areas is caused by the fact that the monitoring process in our experiments does not require any further behavioral adjustments. However, it is yet to be elucidated the exact mechanisms that govern this lateralization pattern.

We also observed significant information flows between centroparietal and frontocentral areas starting as early as 100 ms. This pattern appears before the activation of the network in frontal regions (i.e., between frontocentral and frontolateral), and may be linked to perception processes. Since the cursor moving directions are balanced in both error and correct conditions, this pattern is not correlated with specific moving directions. An interpretation of this frontoparietal interaction is that the sensory representation towards visual perception in the parietal cortex has already been biased by the contents in the working memory, modulating the information flow after stimulus onset, and reported as an integration between bottom-up perception and top-

down control process (Ptak, 2012). However, modulations of connectivity patterns between frontal and parietal regions have not been reported in the studies of monitoring self-generated errors. A previous study was unable to find a significant modulation of phase synchrony between FCz and parietal regions (Cavanagh, Cohen, and Allen, 2009). However, in these studies the EEG data is time-locked to the behavioral responses, and stimulus-locked parietal patterns – more related to sensory processes – may be washed out after trial averaging given the variability of the reaction time.

Besides modulations in the theta band, we also observed decreased connectivity patterns in the beta and gamma bands. The beta band activity is associated with the maintenance of the current sensorimotor or cognitive state (Engel and Fries, 2010). Decreased beta power and beta synchronization are usually related with the changes of cognitive conditions (Pfurtscheller et al., 2005; Jurkiewicz et al., 2006). Also, beta modulation is expressed more strongly if the maintenance of the *status quo* is intended or predicted than after novel or erroneous events (Engel, Fries, and Singer, 2001; Engel and Fries, 2010). Accordingly, greater beta power in frontocentral areas has been reported after correct feedback in reinforcement learning tasks (Cavanagh, Zambrano-Vazquez, and Allen, 2012). This effect has been attributed to increased coactivation of MFC and motor cortices during feedback processing (Cohen and Ranganath, 2007). In turn, other studies reported stronger beta depression and rebound in MEG signals after error trials in a monitoring task (Koelewijn et al., 2008). Together with our results, this shows that the beta modulations are also sensitive to the errors in absence of motor responses. Rather than reflecting low-level automatic motor resonance, the beta desynchronization corresponds to the discontinuation of the current cognitive states as a high level role, not restricted to motor related intentions (Koelewijn et al., 2008; van Schie et al., 2004). This study supports this theory, since no specific movement reaction is required in the task but the continuation of the cognitive state maintenance is no longer sustained after the perception of erroneous events.

Currently, there is an increased interest in the possibility of performing single-trial, spatio-temporal analysis of the neural correlates of monitoring processes (Debener et al., 2005; Cavanagh, Cohen, and Allen, 2009; Heike et al., 2010; Cohen and Cavanagh, 2011; Cavanagh, Zambrano-Vazquez, and Allen, 2012). This allows to elucidate phenomena that are hardly observable using averaging-based methods. Here we show that cross-regional interaction patterns can be estimated at the single-trial level. These patterns are obtained with a regression model, and thus are not linearly dependent with original EEG channels, possibly providing discriminant information for decoding whether a trial corresponds to monitoring the correct or erroneous condition. Notably, significant differences and discrimination capability (Fisher score) in the single trial modulations further verified that the obtained brain interaction patterns during error cognition are coincident with the modulation patterns obtained at the subject level. The estimation of connectivity patterns in a single-trial basis shows that the network dynamics do convey information about the brain modulations of the monitoring process. Importantly, this information is complementary to the one provided by standard ERP analysis for the use of recognizing error trials, both in the temporal and spectral domain.

Recent studies of EEG-based brain-machine interface show that the classification performance of motor imagery tasks using brain connectivity features, either DTF (Billinger, Brunner, and Müller-Putz, 2013) or instantaneous phase difference (Hamner et al., 2011), is comparable to the use of customary band power features. Connectivity-based features have also been used for continuous decoding of arm trajectories from electrocorticography signals showing increased estimation accuracy with respect to spectral features (Benz et al., 2012). However, most of these classification or regression models are mainly data driven, extracting features through optimization algorithms, without providing an explicit interpretation about the selected features. The current work provides evidence that discriminant connectivity-based features not only allow pattern recognition, but are also consistent with the current knowledge about the dynamics of the brain network involved in monitoring processes. Nevertheless, practical applications may consider using the connectivity patterns estimated in the temporal domain (or in narrow-band filtered data). This avoids computing frequency specific components and will reduce the dimensionality of the problem. Further work may be required to assess how much improvement can be expected from this approach.

It should be noticed that the order of the MVAR model is determined by the data using the BIC criterion. In this study, another hard limit comes from the amount of data, $K(p+1)/N_s n_t < 0.1$ (K is the channel number, p is the MVAR order, N_s is the sample number in the time window and n_t is the number of trials) (Korzeniewska et al., 2008), which constrains the order to be smaller than 5.4 in the single-trial analysis. For classification, it is necessary to keep the same order for all the trials, since different MVAR orders may cause a different resolution in the frequency domain, thus resulting in a more arbitrary distribution in the feature space. In addition, the data amount in the analysis window was selected as a trade-off between the sensitivity and the dimensionality of the features, i.e., a larger time window uses higher MVAR order thus more detail in the frequency domain can be obtained, but at the same time leads to a lower resolution (less features) in the temporal domain. Further work should explore alternative algorithms to overcome this limitation, for instance, adaptive DTF based on adaptive estimation of autoregressive parameters (Wilke, Ding, and He, 2008).

To summarize, modulations of brain connectivity patterns appear in both low and high frequency bands in the process of monitoring external events through the recording of scalp EEG. In particular, strong theta modulations are obtained both at average and single-trial levels. These results, consistent with modulations elicited after the monitoring of self-generated errors, support the parsimonious role of theta activity in MFC in coordinating cross-regional activity during various monitoring processes. Importantly, since our protocol does not involve motor response, these network patterns appear to be related to intrinsic mechanisms of the function of error cognition in human brain, instead of being

exclusively linked to co-activation with motor areas. Furthermore, the temporal evolution of the EEG connectivity modulations – i.e., activation of frontoparietal network precedes increased frontolateral interactions – suggests a possibly hierarchical organization of the monitoring cognition: Early frontoparietal interaction may reflect modulation of neural activities by bottom-up sensory inputs, whereas frequency-specific interactions between frontocentral and frontolateral areas reflect the perturbation of cognitive states in the working memory and the preparation for a potential top-down adjustment. Future work will be devoted to investigate the causal dependences between these two modulation patterns, as well as trial-by-trial changes in different response and feedback tasks.

References

Agam, Yigal, Matti S Hämäläinen, Adrian K C Lee, Kara A Dyckman, Jesse S Friedman, Marlisa Isom, Nikos Makris, and Dara S Manoach (2011). Multimodal neuroimaging dissociates hemodynamic and electrophysiological correlates of error processing. *Proc Natl Acad Sci* 108(42): 17556–17561.

Benz, Heather L, Huaijian Zhang, Anastasios Bezerianos, Soumyadipta Acharya, Nathan E Crone, Xioaxiang Zheng, and Nitish V Thakor (2012). Connectivity analysis as a novel approach to motor decoding for prosthesis control. *IEEE Trans Neural Syst Rehabil Eng* 20(2): 143–152.

Billinger, Martin, Clemens Brunner, and Gernot Müller-Putz (2013). Single-trial connectivity estimation for classification of motor imagery data. *J Neural Eng* 10(4): 046006.

Blinowska, Katarzyna J (2011). Review of the methods of determination of directed connectivity from multichannel data. *Med Biol Eng Comput* 49(5): 521–529.

Brázdil, Milan, Claudio Babiloni, Robert Roman, Pavel Daniel, Martin Bares, Ivan Rektor, Fabrizio Eusebi, Paolo Maria Rossini, and Fabrizio Vecchio (2009). Directional functional coupling of cerebral rhythms between anterior cingulate and dorsolateral prefrontal areas during rare stimuli: a directed transfer function analysis of human depth EEG signal. *Hum Brain Mapp* 30(1): 138–146.

Brázdil, Milan, Michal Mikl, Radek Mareucek, Petr Krupa, and Ivan Rektor (2007). Effective connectivity in target stimulus processing: A dynamic causal modeling study of visual oddball task. *Neuroimage* 35: 827–835.

Brown, Joshua W and Todd S Braver (2005). Learned predictions of error likelihood in the anterior cingulate cortex. *Science* 307(5712): 1118–1121.

Buzsáki, György and Andreas Draguhn (2004). Neuronal oscillations in cortical networks. *Science* 304(5679): 1926–1929.

Carter, C. S., A. M. Macdonald, M. Botvinick, L. L. Ross, V. A. Stenger, D. Noll, and J. D. Cohen (2000). Parsing executive processes: strategic vs. evaluative functions of the anterior cingulate cortex. *Proc Natl Acad Sci* 97(4): 1944–1948.

Cavanagh, James F, Michael X Cohen, and John J B Allen (2009). Prelude to and resolution of an error: EEG phase synchrony reveals cognitive control dynamics during action monitoring. *J Neurosci* 29(1): 98–105.

Cavanagh, James F, Laura Zambrano-Vazquez, and John J B Allen (2012). Theta lingua franca: a common mid-frontal substrate for action monitoring processes. *Psychophysiology* 49(2): 220–238.

Chavarriaga, Ricardo and José del R. Millán (2010). Learning from EEG error-related potentials in noninvasive brain-computer interfaces. *IEEE Trans Neural Syst Rehabil Eng* 18(4): 381–388.

Chavarriaga, Ricardo, Aleksander Sobolewski, and José del R. Millán (2014). Errare machinale est: the use of error-related potentials in brain-machine interfaces. *Front Neurosci* 8: 208.

Cohen, Michael X, Nikolai Axmacher, Doris Lenartz, Christian E Elger, Volker Sturm, and Thomas E Schlaepfer (2009). Nuclei accumbens phase synchrony predicts decision-making reversals following negative feedback. *J Neurosci* 29(23): 7591–7598.

Cohen, Michael X and James F Cavanagh (2011). Single-trial regression elucidates the role of prefrontal theta oscillations in response conflict. *Front Psychol* 2: 30.

Cohen, Michael X and Charan Ranganath (2007). Reinforcement learning signals predict future decisions. *J Neurosci* 27(2): 371–378.

Cohen, Michael X, K. Richard Ridderinkhof, Sven Haupt, Christian E Elger, and Juergen Fell (2008). Medial frontal cortex and response conflict: evidence from human intracranial EEG and medial frontal cortex lesion. *Brain Res* 1238: 127–142.

de Bruijn, Ellen R A, Floris P Lange, D. Yves Cramon, and Markus Ullsperger (2009). When errors are rewarding. *J Neurosci* 29(39): 12183–12186.

Debener, Stefan, Markus Ullsperger, Markus Siegel, Katja Fiehler, D. Yves Cramon, and Andreas K Engel (2005). Trial-by-trial coupling of concurrent electroencephalogram and functional magnetic resonance imaging identifies the dynamics of performance monitoring. *J Neurosci* 25(50): 11730–11737.

Engel, A. K., P. Fries, and W. Singer (2001). Dynamic predictions: oscillations and synchrony in top-down processing. *Nat Rev Neurosci* 2(10): 704–716.

Engel, Andreas K and Pascal Fries (2010). Beta-band oscillations–signalling the status quo? *Curr Opin Neurobiol (Lond)* 20(2): 156–165.

Ferrez, Pierre W. and José del R. Millán (2008). Error-related EEG potentials generated during simulated brain-computer interaction. *IEEE Trans Biomed Eng* 55: 923–929.

Gehring, W. J., B. Goss, M. G. H. Coles, D. E. Meyer, and E. A. Donchin (1993). Neural system for error-detection and compensation. *Psychol Sci* 4: 385–90.

Gevins, A. and M. E. Smith (2000). Neurophysiological measures of working memory and individual differences in cognitive ability and cognitive style. *Cereb Cortex* 10(9): 829–839.

Grosse-Wentrup, M., C. Liefhold, K. Gramann, and M. Buss (2009). Beamforming in noninvasive brain computer interfaces. *IEEE Trans Biomed Eng* 56(4): 1209–1219.

Hamner, Benjamin, Robert Leeb, Michele Tavella, and José del R. Millán (2011). Phase-based features for motor imagery brain-computer interfaces. *Conf Proc IEEE Eng Med Biol Soc* 2011: 2578–2581.

Heike, Eichele, Juvodden Hilde, Ullsperger Markus, and Eichele Tom (2010). Maladaptation of event-related EEG responses preceding performance errors. *Front Hum Neurosci* 4(0): 12.

Hipp, Joerg F, Andreas K Engel, and Markus Siegel (2011). Oscillatory synchronization in large-scale cortical networks predicts perception. *Neuron* 69(2): 387–396.

Holroyd, Clay B and Michael G H Coles (2002). The neural basis of human error processing: Reinforcement learning, dopamine, and the error-related negativity. *Psychol Rev* 109(4): 679–709.

Holroyd, Clay B, Sander Nieuwenhuis, Nick Yeung, Leigh Nystrom, Rogier B Mars, Michael G H Coles, and Jonathan D Cohen (2004). Dorsal anterior cingulate cortex shows fMRI response to internal and external error signals. *Nat Neurosci* 7(5): 497–498.

Iturrate, I., R. Chavarriaga, L. Montesano, J. Minguez, and José del R. Millán (2014). Latency correction of event-related potentials between different experimental protocols. *J Neural Eng* 11(3): 036005.

Jurkiewicz, Michael T, William C Gaetz, Andreea C Bostan, and Douglas Cheyne (2006). Post-movement beta rebound is generated in motor cortex: evidence from neuromagnetic recordings. *Neuroimage* 32(3): 1281–1289.

Kamiński, M., M. Ding, W. A. Truccolo, and S. L. Bressler (2001). Evaluating causal relations in neural systems: Granger causality, directed transfer function and statistical assessment of significance. *Biol Cybern* 85(2): 145–157.

Kamiński, M. J. and K. J. Blinowska (1991). A new method of the description of the information flow in the brain structures. *Biol Cybern* 65(3): 203–210.

Kayser, Jrgen and Craig E. Tenke (2006). Principal components analysis of laplacian waveforms as a generic method for identifying ERP generator patterns: I. evaluation with auditory oddball tasks. *Clin Neurophysiol* 117(2): 348 – 368.

Kerns, John G, Jonathan D Cohen, Angus W MacDonald, Raymond Y Cho, V. Andrew Stenger, and Cameron S Carter (2004). Anterior cingulate conflict monitoring and adjustments in control. *Science* 303(5660): 1023–1026.

Klimesch, W. (1999). EEG alpha and theta oscillations reflect cognitive and memory performance: a review and analysis. *Brain Res Rev* 29(2-3): 169–195.

Klimesch, W., M. Doppelmayr, A. Yonelinas, N. E. Kroll, M. Lazzara, D. Rhm, and W. Gruber (2001). Theta synchronization during episodic retrieval: neural correlates of conscious awareness. *Cogn Brain Res* 12(1): 33–38.

Koelewijn, Thomas, Hein T Schie, Harold Bekkering, Robert Oostenveld, and Ole Jensen (2008). Motor-cortical beta oscillations are modulated by correctness of observed action. *Neuroimage* 40(2): 767–775.

Korzeniewska, Anna, Ciprian M Crainiceanu, Rafaf Kuś, Piotr J Franaszczuk, and Nathan E Crone (2008). Dynamics of event-related causality in brain electrical activity. *Hum Brain Mapp* 29(10): 1170–1192.

Kuwabara, Masaru, Farshad A Mansouri, Mark J Buckley, and Keiji Tanaka (2014). Cognitive control functions of anterior cingulate cortex in macaque monkeys performing a wisconsin card sorting test analog. *J Neurosci* 34(22): 7531–7547.

Luks, Tracy L, Gregory V Simpson, Robert J Feiwell, and William L Miller (2002). Evidence for anterior cingulate cortex involvement in monitoring preparatory attentional set. *Neuroimage* 17(2): 792–802.

Luu, P., T. Flaisch, and D. M. Tucker (2000). Medial frontal cortex in action monitoring. *J Neurosci* 20(1): 464–469.

Mazaheri, Ali, Ingrid L C Nieuwenhuis, Hanneke Dijk, and Ole Jensen (2009). Prestimulus alpha and mu activity predicts failure to inhibit motor responses. *Hum Brain Mapp* 30(6): 1791–1800.

Milner, W. H. R., J. Brauer, H. Hecht, R. Trippe, and M. G. H. Coles (2004). Parallel brain activity for self-generated and observed errors. *Errors, Conflicts, and the Brain. Current Opinions on Performance Monitoring* pp. 124–129.

Oya, Hiroyuki, Paul W F Poon, John F Brugge, Richard A Reale, Hiroto Kawasaki, Igor O Volkov, and Matthew A Howard (2007). Functional connections between auditory cortical fields in humans revealed by granger causality analysis of intra-cranial evoked potentials to sounds: comparison of two methods. *Biosystems* 89(1-3): 198–207.

Pfurtscheller, G., C. Neuper, C. Brunner, and F. Lopes Silva (2005). Beta rebound after different types of motor imagery in man. *Neurosci Lett* 378(3): 156–159.

Ptak, Radek (2012). The frontoparietal attention network of the human brain: action, saliency, and a priority map of the environment. *Neuroscientist* 18(5): 502–515.

Sauseng, Paul, Wolfgang Klimesch, Michael Doppelmayr, Simon Hanslmayr, Manuel Schabus, and Walter R Gruber (2004). Theta coupling in the human electroencephalogram during a working memory task. *Neurosci Lett* 354(2): 123–126.

Schneider, Tapio and Arnold Neumaier (2001). Algorithm 808: Arfit - a matlab package for the estimation of parameters and eigenmodes of multivariate autoregressive models. *ACM T Math Software* 27(1): 58–65.

Schoffelen, Jan-Mathijs and Joachim Gross (2009). Source connectivity analysis with MEG and EEG. *Hum Brain Mapp* 30(6): 1857–1865.

Shane, Matthew S, Michael Stevens, Carla L Harenski, and Kent A Kiehl (2008). Neural correlates of the processing of another's mistakes: a possible underpinning for social and observational learning. *Neuroimage* 42(1): 450–459.

Taylor, Stephan F, Emily R Stern, and William J Gehring (2007). Neural systems for error monitoring: Recent findings and theoretical perspectives. *Neuroscientist* 13(2): 160–172.

Trujillo, Logan T and John J B Allen (2007). Theta EEG dynamics of the error-related negativity. *Clin Neurophysiol* 118(3): 645–668.

Tsujimoto, Toru, Hideki Shimazu, Yoshikazu Isomura, and Kazuo Sasaki (2010). Theta oscillations in primate prefrontal and anterior cingulate cortices in forewarned reaction time tasks. *J Neurophysiol* 103(2): 827–843.

Ullsperger, M. and D. Y. Cramon (2001). Subprocesses of performance monitoring: a dissociation of error processing and response competition revealed by event-related fMRI and ERPs. *Neuroimage* 14(6): 1387–1401.

Ullsperger, Markus, Adrian G Fischer, Roland Nigbur, and Tanja Endrass (2014). Neural mechanisms and temporal dynamics of performance monitoring. *Trends Cogn Sci* 18(5): 259–267.

van Schie, Hein T, Rogier B Mars, Michael G H Coles, and Harold Bekkering (2004). Modulation of activity in medial frontal and motor cortices during error observation. *Nat Neurosci* 7(5): 549–554.

Vanderhasselt, Marie-Anne, Rudi De Raedt, and Chris Baeken (2009). Dorsolateral prefrontal cortex and stroop performance: tackling the lateralization. *Psychon Bull Rev* 16(3): 609–612.

Wang, Chunmao, Istvan Ulbert, Donald L Schomer, Ksenija Marinkovic, and Eric Halgren (2005). Responses of human anterior cingulate cortex microdomains to error detection, conflict monitoring, stimulus-response mapping, familiarity, and orienting. *J Neurosci* 25(3): 604–613.

Wilke, Christopher, Lei Ding, and Bin He (2008). Estimation of time-varying connectivity patterns through the use of an adaptive directed transfer function. *IEEE Trans Biomed Eng* 55(11): 2557–2564.

Womelsdorf, Thilo, Kevin Johnston, Martin Vinck, and Stefan Everling (2010). Theta-activity in anterior cingulate cortex predicts task rules and their adjustments following errors. *Proc Natl Acad Sci* 107(11): 5248–5253.

Highlights

- Analysis of error-related brain connectivity patterns in multiple and single-trial
- Increased θ and decreased β connectivity in fronto-parietal during error monitoring
- Prove frontal theta as a common mechanism for different monitoring cognitions.
- Cross-regional interaction patterns convey information at single-trial levels